AIP | Journal of Applied Physics

# Realization of In0.75Ga0.25As two-dimensional electron gas bilayer system for spintronics devices based on Rashba spin-orbit interaction

M. Akabori, S. Hidaka, H. Iwase, S. Yamada, and U. Ekenberg

Citation: J. Appl. Phys. **112**, 113711 (2012); doi: 10.1063/1.4766749
View online: http://dx.doi.org/10.1063/1.4766749
View Table of Contents: http://jap.aip.org/resource/1/JAPIAU/v112/i11
Published by the American Institute of Physics.

JOURNAL OF APPLIED PHYSICS **112**, 113711 (2012)

# Realization of $In_{0.75}Ga_{0.25}As$ two-dimensional electron gas bilayer system for spintronics devices based on Rashba spin-orbit interaction

M. Akabori,[1] S. Hidaka,[1] H. Iwase,[1] S. Yamada,[1,a)] and U. Ekenberg[2]
[1]*Center for Nano Materials and Technology (CNMT), Japan Advanced Institute of Science and Technology (JAIST), 1-1, Asahi-dai, Nomi, Ishikawa 923-1292, Japan*
[2]*School of Information and Communication Technology, Royal Institute of Technology (KTH), SE-16440 Kista, Sweden*

(Received 5 July 2012; accepted 17 October 2012; published online 10 December 2012)

Narrow gap InGaAs two-dimensional electron gas (2DEG) bilayer samples are fabricated and confirmed to have good electronic qualities as well as strong Rashba-type spin-orbit interactions (SOIs). The 2DEG systems are realized by molecular beam epitaxy in the form of wide quantum wells (QWs) with thicknesses $t_{QW} \sim 40$–$120$ nm modulation doped in both the upper and lower InAlAs barriers. From the Hall measurements, the overall mobility values of $\mu_e \sim 15$ m$^2$/V s are found for the total sheet electron density of $n_s \sim 8 \times 10^{11}$/cm$^2$, although the $n_s$ is distributed asymmetrically as about 1:3 in the upper and lower 2DEGs, respectively. Careful low temperature magneto-resistance analysis gives large SO coupling constants of $\alpha \sim 20 \times 10^{-12}$ eV m as well as expected electron effective masses of $m^*/m_0 \sim 0.033$-$0.042$ for each bilayer 2DEG spin sub-band. Moreover, the enhancement of $\alpha$ with decrease of $t_{QW}$ is found. The corresponding self-consistent calculation, which suggests the interaction between the bilayer 2DEGs, is carried out and the origin of $\alpha$ enhancement is discussed.
 [http://dx.doi.org/10.1063/1.4766749]

## I. INTRODUCTION

Semiconductor spintronics[1] is a highly attractive research area from the viewpoints of fundamental physics as well as of future electronic/optic device applications. As typical candidate basic materials to be utilized in those researches, (dilute) magnetic semiconductors (DMSs)[2] and non-magnetic semiconductors/hetero-structures have usually been proposed and studied. In order to manipulate spins of fixed and/or conducting electrons, fixed magnetic atoms play a major role in the former material. However, in the latter case, some special effects which control spins in a particular material or hetero-structure are necessary.

One model device in non-magnetic semiconductor spintronics is the so-called Datta-Das spin field-effect-transistor (FET),[3] where the specific effect is a Rashba-type spin-orbit interaction (SOI)[4] originated from the structure-induced *asymmetry* (SIA) in the hetero-structures. Due to this effect, (two-dimensional) electrons travelling (in the velocity of $\boldsymbol{v_x}$) along the *asymmetric* potential interface (of local electric field, $\boldsymbol{E_y}$) make spin precession around the axis of effective magnetic field, $\boldsymbol{B_z} \propto \boldsymbol{v_x} \times \boldsymbol{E_y}$. The sensitivity of the precession angle is defined as a spin-orbit coupling constant, $\alpha$, which is proportional to the expectation value of the interface electric field, $\langle \boldsymbol{E_y} \rangle$.

In order to realize this kind of device, it is necessary to select semiconductor hetero-structures which can have both a two-dimensional electron gas (2DEG) with a gate controllable strong SOI and a ferromagnetic (FM) electrode with a high spin-injection/detection efficiency. The latter should be formed on top or side of the hetero-structure surface with an easy fabrication process. Since $\alpha$ is also roughly proportional to $1/m^*\varepsilon_g$ ($m^*$: 2DEG electron effective mass, $\varepsilon_g$: band gap), there have so far been proposed a variety of *narrow gap* material hetero-structures such as HgTe/CdTe,[5] InGaAs/InAlAs,[6,7] InGaAs/InP,[8] InAs based,[9] and InGaSb/InAlSb.[10] The first problem is mostly solved in some materials, where the gate controllable $\alpha$ values of $\leq 20 \times 10^{-12}$ eV m are obtained.[7,9] However, a high efficient spin injection electrode by popular magnetic metals or alloys, has not been found for any hetero-junction systems. In addition, alternative trials to use dilute semiconductors or spin Hall effect (SHE)[11,12] parts as spin injectors have not succeeded yet. For example, typical DMSs, GaMnAs, or InMnAs are usually p-type and difficult to be hybridized with the above hetero-junctions by usual epitaxial growth or device process technologies. The SHE, which is expected to have a universal spin conductance of $e/8\pi$ in pure electron system,[12] is later found to be entirely suppressed by impurity damping.[13]

But, one important thing to be noted here is that those difficulties are some extent related to the fact that the materials proposed so far for the spin-FET are all 2DEG *monolayer* systems. In fact, recently, several advantages of utilizing 2DEG *bilayer* in the "spintronics based on the Rashba effect (Rashba spintronics)" are proposed mainly from the theoretical points of view: Gvozdic and Ekenberg pointed out[14] that the modulation-doped wide quantum well (QW) structure has a larger $\langle \boldsymbol{E_y} \rangle$ at both the interfaces giving enhanced SOI. As for the new device proposal, an asymmetric wide QW structure is expected to act as a spin switch[15] due to the anti-cross coupling between the spin dispersions

$$\varepsilon_{\uparrow\downarrow} = \hbar^2 k_{\uparrow\downarrow}^2 / 2m* \pm \alpha k_{\uparrow\downarrow},$$

a)Author to whom correspondence should be addressed. Electronic mail: shooji@jaist.ac.jp.

 

of the 2DEGs localized at both the interfaces but interacting loosely with each other. The vertical type device, so called spin "resonant tunneling diode"[16] acting as a spin filter has also been proposed. Moreover, a quasi interference ring can be formed by the 2DEG bilayer and the non-magnetic two-terminal electrodes,[17] which could open a field of "interference transistors" again based on Aharonov-Bohm (AB)[18] and/or Aharonov-Casher (AC)[19] effects. Particularly, no measurement reports have been done as for the *vertical* AC rings.

Related to the spin-injection, the theory of SHE in a bilayer electron gas[20] should be paid much more attention. They have found that "resonant magnification" of the SHE can occur due to the cross coupling similar to that mentioned above and the magnified SHE has possibly been robust from the impurity damping. In other words, only in the bilayer 2DEG systems with strong Rashba SOI, the Datta-Das spin-FET with SHE spin-injection electrodes could be realized. Thus, the bilayer 2DEG which reveals strong Rashba effect has many promising features, but there have so far been almost no reports relating to the fabrication, transport analysis, and hence application of such a 2DEG bilayer system.

In this article, we report the fabrication and the detailed analysis results of the 2DEG bilayers realized in a form of $In_{0.75}Ga_{0.25}As/In_{0.75}Al_{0.25}As$ modulation-doped wide QW structures. The samples with different QW widths of $t_{QW} = 40$–$120$ nm, the layered structure of which is shown in Fig. 1, have been grown by molecular beam epitaxy (MBE). Then, sheet electron density $n_s$, effective mass $m^*$, and SO coupling constant $\alpha$ are successfully estimated for each

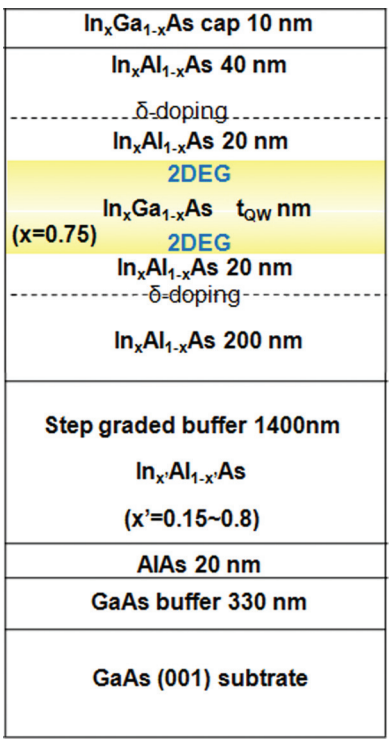


FIG. 1. Schematic layered structure of 2DEG bilayer sample realized in the form of modulation-doped wide InGaAs quantum well. Nominal In content in the 2DEG heterostructure is 0.75. $\delta$-doping condition is identical to be $\sim 6 \times 10^{11}/cm^2$ for both the 2DEGs. InGaAs well widths are 40, 60, 80, 100, and 120 nm.

2DEG spin sub-band located at the both interfaces via variable temperature magneto-resistance (MR) measurements. The changes of $m^*$ with decreasing $t_{QW}$ and the enhancements of $\alpha$ for the smaller $t_{QW}$ are confirmed. Thus, it is discussed the possibility that the interactions between the upper and lower 2DEGs give such results depending on $t_{QW}$. In order to make the discussion even more quantitatively, the self-consistent calculation of potential and 2DEG spatial distributions in those wide QW samples is carried out.

## II. SAMPLE PREPARATION AND EXPERIMENTAL

The 2DEG bilayer samples are grown by conventional solid-source MBE. The layer structure from the top is as follows: $In_{0.75}Ga_{0.25}As$ cap (10 nm), $In_{0.75}Al_{0.25}As$ (40 nm), Si $\delta$-doping, $In_{0.75}Al_{0.25}As$ spacer (20 nm), $In_{0.75}Ga_{0.25}As$ well (widths, $t_{QW}$), $In_{0.75}Al_{0.25}As$ spacer (20 nm), Si $\delta$-doping, $In_{0.75}Al_{0.25}As$ (200 nm), $In_xAl_{1-x}As$ step-graded buffer (1400 nm, $x = 0.15$–$0.8$, increment $\Delta x = 0.05$, 100 nm step), AlAs buffer (20 nm), and GaAs buffer (30 nm) on semi-insulating GaAs (001) substrate. The upper and lower Si $\delta$-doping conditions are identical to be $6 \times 10^{11}/cm^2$. The wafers have typical cross hatch pattern on their surfaces usual for the metamorphic epitaxial growth.

MR measurements have been performed at temperatures of 1.5–20 K using the AC lock-in method in a $^4$He cryostat with 8 T superconductive magnet. Hall bar samples with the width of 50 $\mu$m and the distance between the probes of 200 $\mu$m were fabricated, and those with the current direction parallel to [-110] are mainly measured, since the 2DEG mobility is anisotropic and higher in this planar direction.

In the usual analysis of *mono*layer 2DEG with Rashba SOI, the low field part of longitudinal resistivity ($\rho_{xx}$) oscillation (or the derivative) is Fourier transformed and the sheet electron densities ($n_{s\uparrow}$ *and* $n_{s\downarrow}$) for the spin subbands are determined, if the peak splits due to the SOI. The SO coupling constant is then estimated[8] using the equation, $\alpha_{FFT} = (\Delta n_s \hbar^2/m*)(\pi/2(n_s - \Delta n_s))^{1/2}$, where $n_s = n_{s\uparrow} + n_{s\downarrow}$ *and* $\Delta n_s = n_{s\downarrow} - n_{s\uparrow}$. This can be cross checked by the period of beating signal $(\Delta i/\Delta(B^{-1}))$ corresponding to the split Fourier peak via the equation, $\alpha_{beat} = (e\hbar/2m^* k_F)(\Delta i/\Delta(B^{-1}))$, where $i$ is the node number. However, in the bilayer samples, there are at least two 2DEG sub-bands most possibly belonging to the upper and lower 2DEGs and an additional oscillation such as magneto inter-subband scattering (MIS) oscillation[21] could appear together with the Shubnikov de-Haas (SdH) ones. Thus, we often have *several* peaks in the Fourier spectrum for the MR signal in the bilayer samples. This brings the difficulty in identifying the peaks corresponding to the SdH oscillation of each 2DEG. If one fails to make those identifications, it then becomes impossible to estimate $\alpha$ s *for each* 2DEG from the Fourier peak splitting and/or beating signal of the oscillation.

We here adopted variable temperature analysis with inverse Fourier transformation technique. Here, the SdH oscillations are measured at low temperatures ($\sim$20 K) in the form of longitudinal magneto-resistance signal and the main (two) Fourier peaks of the SdH oscillation are separated and then reverse Fourier transformed individually to reproduce

original oscillations corresponding to the peaks. Temperature variations of the reproduced oscillation amplitude were fitted by the theory of approximate SdH oscillations to estimate the electron effective mass at the Fermi level of the 2DEG. Since the MIS oscillation amplitude is believed to have a different temperature dependency[22] compared with the SdH case, this type analysis may be effective to distinguish the SdH signal and the MIS oscillation. Moreover, the separate reproductions of oscillations make it easy to identify the beating signal relating to the SOI. The genuine SO coupling constants $\alpha$ s are indeed deduced by careful analysis of the temperature dependent spin-split Fourier peaks and corresponding beat signals. As shown later, they are found to become dominant over MIS oscillation at moderate temperatures close to 20 K. The effective masses deduced for the each 2DEG are crucial, since they should be used to determine the correct $\alpha$ individually for the each sub-band. We often see the risky use of band edge mass value in the determination, which might result in a large over-estimation of $\alpha$.

## III. RESULTS AND DISCUSSIONS

We have analyzed five samples with different $In_{0.75}Ga_{0.25}As$ well widths, $t_{QW} = 40$–120 nm. Van der Pauw measurements give us the rough results of total $n_s \sim 8 \times 10^{11}/cm^2$ and $\mu_e \leq 1.5 \times 10^5$ $cm^2/V$ s at ~4 K for those samples. Figure 2, upper panel, shows magneto and Hall resistivities ($\rho_{xx}$ and $\rho_{xy}$) of the five samples. As seen in the figure, non-monotonic and complicated oscillations are obtained for $\rho_{xx}$ at low fields, while at high fields $\rho_{xx}$ often approaches to zero values especially for small $t_{QW}$ (40 and 60 nm) samples. Corresponding to those zero bottoms, almost flat quantum Hall plateaus are observed in $\rho_{xy}$. Those features indeed suggest the high electronic qualities of the samples. However, as mentioned above, a simple spectrum analysis of $\rho_{xx}$ is not enough to deduce the sheet electron densities or the SO coupling constants ($\alpha$ s) for each 2DEG sub-band in the 2DEG bilayer systems. As an additional part of the MR measurements, we also confirmed weak anti-localization (WAL) signals[23] (Fig. 2, lower panel) in the conductivity in the vicinity of $B \sim 0$. Although the data suggest the existence of SOI in all the samples, they are useless for estimating $\alpha$ values for each 2DEG due to the lack of fitting theory for the bilayer system. However, the WAL peak height as well as the field of minima seem to increase with the decrease of $t_{QW}$, which might be a sign of the SOI enhancements in the narrow well samples.

We then differentiate twice the $\rho_{xx}$ signals of 0–3 T in Fig. 2, upper panel, and applied fast Fourier transform analysis. We then obtained Fourier spectrum as shown in Fig. 3, upper panel, for $t_{QW} = 80$ nm case. Here, we observed three

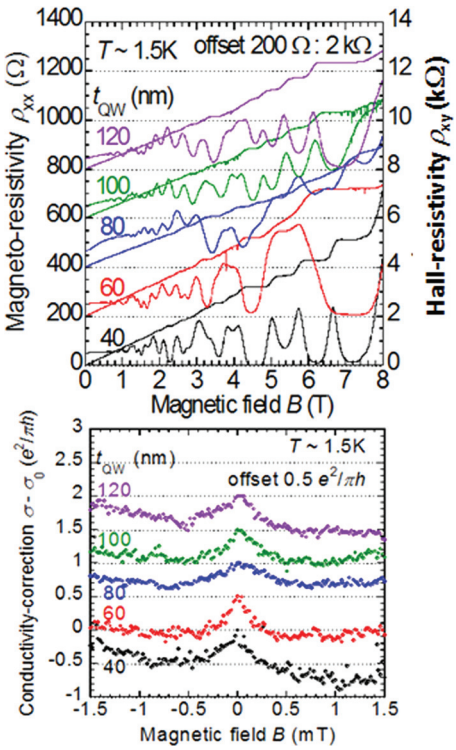


FIG. 2. (Upper panel) Magneto- and Hall resistivities ($\rho_{xx}$ and $\rho_{xy}$) in five samples measured at 1.5 K up to 8 T. In $\rho_{xx}$, we can see SdH oscillations complicated due to the 2DEG occupation in several (spin) sub-bands. But, in the samples with narrower InGaAs wells of 40 and 60 nm, $\rho_{xx} \sim 0$ bottoms and corresponding $\rho_{xy}$ plateaus were observed. (Lower panel) Weak anti-localization signals observed in the five samples at the vicinity of $B \sim 0$.

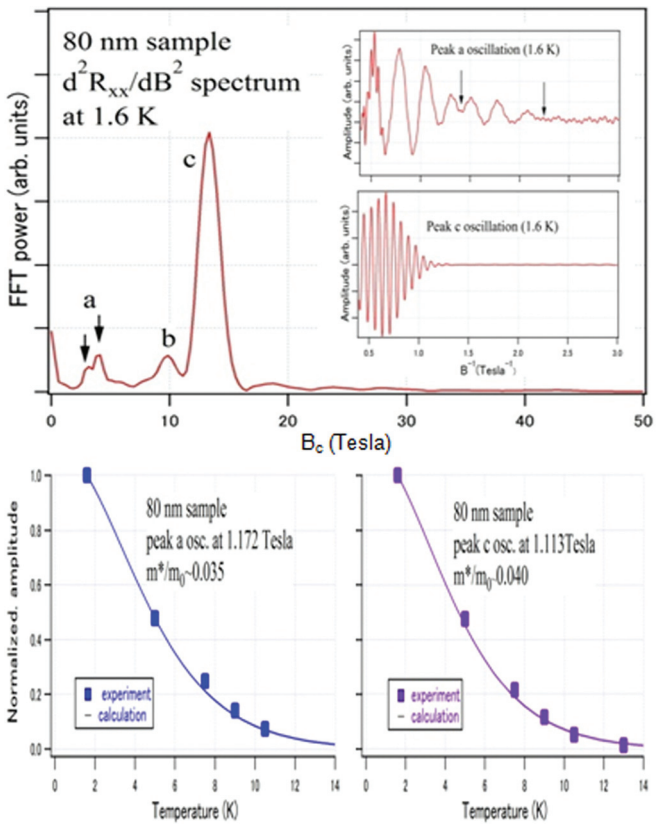


FIG. 3. (Upper panel) FFT spectrum of the $d^2\rho_{xx}/dB^2$ oscillation for the $t_{QW} = 80$ nm sample deduced from $\rho_{xx}$ (within 0–3 T) shown in Fig. 2, upper panel. Inset: reproduced $d^2\rho_{xx}/dB^2$ oscillations for the peak **a** (upper) and peak (**b** + **c**) (lower), respectively, via inverse Fourier transform. Here, corresponding to the splitting in the peak **a**, the beat signal is observed in the oscillation in the upper panel. (Lower panels) Fitting results by the theory for the temperature dependencies of the amplitudes of the oscillations in the upper panel are shown in lower left and lower right panels for the upper and lower 2DEGs, respectively. Electron effective masses described in the figures are the values determined for the each 2DEG.

TABLE I. Sub-band parameters determined in the present article for five samples with different well thicknesses ($t_{QW}$s). **α** s for upper 2DEGs in the samples 2, 4, and 5 were not able to be determined due to the lack of FFT peak splitting.

| Sample No. | 1 | 2 | 3 | 4 | 5 |
|---|---|---|---|---|---|
| Well thickness, $t_{QW}$ (nm) | 40 | 60 | 80 | 100 | 120 |
| $n_s$ (upper 2DEG) ($\times 10^{11}$/cm$^2$) | 1.76 ± 0.2 | 1.61 ± 0.2 | 1.76 ± 0.2 | 1.46 ± 0.2 | 1.46 ± 0.2 |
| $n_s$ (lower 2DEG) ($\times 10^{11}$/cm$^2$) | 5.76 ± 0.3 | 6.07 ± 0.3 | 5.76 ± 0.3 | 6.34 ± 0.3 | 6.22 ± 0.3 |
| m*/$m_0$ (upper 2DEG) | 0.032 ± 0.001 | 0.034 ± 0.001 | 0.035 ± 0.001 | 0.035 ± 0.001 | 0.036 ± 0.001 |
| m*/$m_0$ (lower 2DEG) | 0.041 ± 0.001 | 0.038 ± 0.001 | 0.039 ± 0.001 | 0.040 ± 0.001 | 0.039 ± 0.001 |
| α (upper 2DEG) ($\times 10^{-12}$ eV m) | 23.6 ± 2 | … | 17.6 ± 2 | … | … |
| α (lower 2DEG) ($\times 10^{-12}$ eV m) | 24.3 ± 3 | 20.7 ± 3 | 25.5 ± 3 | 18.5 ± 3 | 19.4 ± 3 |

peaks of **a**, **b**, and **c**, and those are identified to be corresponding to upper 2DEG, MIS oscillation, and lower 2DEG, respectively. The reason of the identifications of peak **a** and **c** is that we confirmed the disappearance of peak **a** by applying negative voltage to the top-gated sample and also the appearance of peak **a** by illuminating a dark sample by visible light. The characteristic field of peak **b** is found to be the difference of the peaks **a** and **c**, suggesting the correctness of the peak **b** identification as MIS. Thus, for the upper and lower 2DEGs, $n_s$ s are estimated to be ~2 and ~$6 \times 10^{11}$/cm$^2$ from Fourier peaks, respectively, as seen in Table I, although the modulation-doping conditions are identical.

The insets in Fig. 3, upper panel, are the reproduced SdH oscillations for the upper and lower 2DEGs, respectively, obtained by the inverse Fourier transformation of peak **a** and **b** + **c** separately. The amplitude variations of the oscillations are plotted against temperature in Fig. 3, lower left and right panels. Thin lines are the fitting curves

$$A(T)/A(T_0) \sim T \sinh(\beta T_0/B)/T_0 \sinh(\beta T_0/B),$$

deduced based on the approximate equation[24] of the SdH oscillation, where $T_0$ is the bottom temperature and $\beta = 2\pi^2 k_B m^*/\hbar e$. From this fitting, we can determine the electron effective mass at the Fermi level for the corresponding 2DEG. We here obtained for $t_{QW} = 80$ nm sample m*/m ~ 0.035 and 0.040 for the upper and lower 2DEGs, respectively. Those m* values seem very reasonable, if we refer the former cyclotron resonance results[25] for the appropriate $n_s$ monolayer 2DEG sample and the band nonparabolicity together with the Fermi level difference between the 2DEGs. This estimation result also supports the correctness of our Fourier peak identifications.

The SO coupling constant, **α**, is determined by the splitting of individual Fourier peak and/or by the beat signal appeared in the reproduced SdH oscillations. In the case of $t_{QW} = 80$ nm sample, peak **a** in Fig. 3, upper panel, splits and the value of **α** ~$18 \times 10^{-12}$ eVm is obtained for the upper 2DEG. While **α** could not be derived for the lower 2DEG from the data shown in Fig. 3, upper panel, since we observed neither splitting in the Fourier peak nor beat signal in the oscillation. We then analyzed the variable temperature data very carefully. Figure 4 shows temperature dependent Fourier spectra (left panel) of the second derivative MR within B = 0–3 T and the corresponding SdH oscillations (right panel) reproduced from the spectra within $B_c$ = 7–30 T (peaks **b**, **b′**, and **c** are included) in the sample of $t_{QW} = 120$ nm. In the left panel of the figure, the behaviors of peaks **b** and **b′** should be focused on. The peak **b**, which corresponds probably to the MIS oscillation (note that $B_c(b) \sim B_c(c) - B_c(a)$), seems to decrease and then the peak **b′** increases with the increase of temperature. The difference between $B_c(\mathbf{b}') \sim B_c(\mathbf{b})$ is very small but finite in this sample. However, if we look at the temperature dependence of the oscillation (right panel), it is found that a beat signal at 1.7 K almost disappears at ~8 K and then a different and

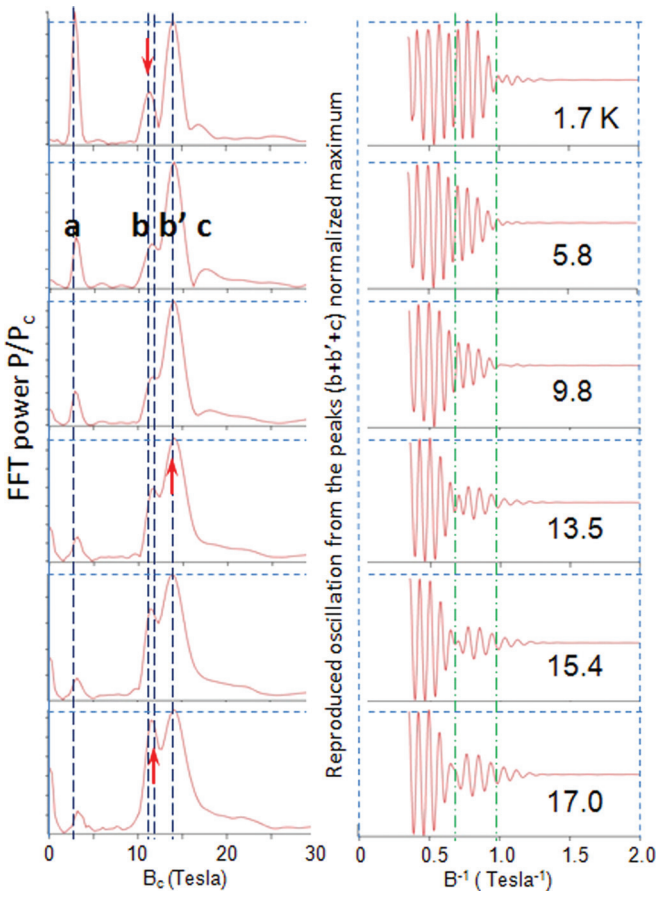


FIG. 4. Temperature dependent FFT spectra of $d^2\rho_{xx}/dB^2$ (normalized by the peak **c** height, left panel) and corresponding oscillations reproduced from the peak (**b** + **b′** + **c**) via inverse FFT (normalized by the maximum amplitude, right panel) in the $t_{QW} = 120$ nm sample. A peak **b** appeared at 1.7 K almost decays at ~7 K and a new peak **b′** slightly shifted reveals and grows at higher temperatures in the left panel. Corresponding to the peak behaviors, two kinds of beating signals are appearing when the temperature increases in the right panel. Similar behaviors are commonly observed in all the five samples making it possible to estimate an accurate **α** in the lower 2DEG.

stronger beat signal grows from ~10 K. This means that the MIS signal seen at the bottom temperature disappears quickly and then a new signal masked initially by the MIS becomes dominant at higher temperatures. Since the peak height of peak **b′** almost reaches to that of peak **c** at higher temperatures, we conclude that this peak and peak **c** represent the correct spin splitting of the lower 2DEG. Similar behaviors are confirmed also for the other samples with different $t_{QW}$s. The reason of this behavior is probably twofold: First is the relatively rapid damping of the upper 2DEG oscillation due to the low mobility, which helps the quick disappearance of the MIS peak. Second is the kind of averaging due to the suppression of inter spin-subband scattering. We thus deduced **α** s of the lower 2DEGs from such a style analysis. Of course, we here used $m^*/m_0$ values of ~0.035 and ~0.040, for the upper and lower 2DEGs, respectively, deduced experimentally in each sample.

Table I summarizes the sheet electron densities ($n_s$s), electron effective masses ($m^*/m_0$ s), and spin-orbit coupling constants (α s) in the 2DEGs (spin sub-bands) obtained in the present analysis and Figure 5 shows the well width ($t_{QW}$) dependency of the quantities related to the three important parameters. From this table and Fig. 5, we can confirm that $n_s$ of upper 2DEG increases, while that of lower 2DEG decreases with the decrease of $t_{QW}$ and the total is kept almost constant. Electron effective mass, $m^*/m_0$, at the Fermi level seems to be *decreasing* for the upper 2DEG and almost constant for the lower 2DEG, when $t_{QW}$ decreases. The dependency of the upper 2DEG mass is not easily acceptable, if we see only the $n_s$ *increase* with the decrease of $t_{QW}$, since the higher $n_s$ usually leads to a heavier 2DEG mass due to the band non-parabolicity. SO coupling constants, α s, of $\sim 20 \times 10^{-12}$ eV m, which are as high as the largest values ever obtained so far,[7,9] are indeed confirmed for almost all cases, although the error bars are to some extent large due to the averaging for several samples. It is interesting that they are likely increasing with the decrease of $t_{QW}$. This behavior seems reliable, since the WAL measurement described earlier also suggests the enhancement of SOI in the narrow well samples.

In order to discuss and find the reason of the $t_{QW}$ dependencies of those parameters, especially $m^*/m_0$ and α, we show in Fig. 6, left panel, the results of self-consistent calculations for the 2DEG bilayer system samples. In the calculation, we have assumed materials parameters estimated by Vegard's law and an asymmetric doping condition which nearly gives the experimental $n_s$ values in the $t_{QW} = 120$ nm sample. We should here pay attention that electron distributions, $|\Psi|^2$, of the upper 2DEG expand to the inside of the well from the upper interface, especially for the narrower QW samples, due to the asymmetric and relatively low potential barrier at the center of the well, although the lower 2DEGs have mostly similar spatial distribution localized at the lower interface. This could be a major reason for the lighter mass of the upper 2DEG in the narrower QW samples.

We next consider the possible reason of α enhancements in the narrower QWs. Since in our system the directions of electric field ($\boldsymbol{E}_y$) and hence those of effective magnetic field ($\boldsymbol{B}_z$) are opposite between the upper and lower 2DEGs, the spin precession directions also become opposite. In such a case, if the 2DEGs are fully symmetric ($n_s$ (upper 2DEG) = $n_s$ (lower 2DEG) and the 2DEGs have the same α),

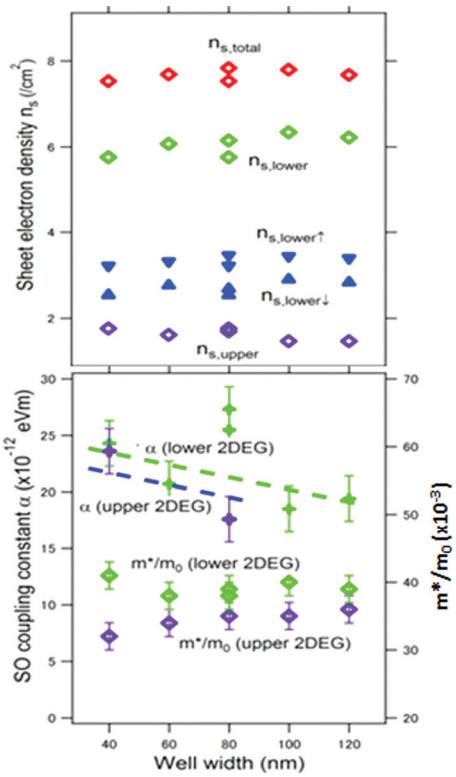


FIG. 5. (Upper panel) Well width ($t_{QW}$) dependency of various sheet electron densities, $n_{s,total} = n_{s,upper\ (2DEG)} + n_{s,lower\ (2DEG)}$, $n_{s,lower\ (2DEG)} = n_{s,lower}\uparrow_{(up\ spin)} + n_{s,lower}\downarrow_{(down\ spin)}$ determined by the FFT analysis of temperature dependent SdH oscillations. (Lower panel) Well width ($t_{QW}$) dependency of electron effective mass ($m^*/m_0$) and SO coupling constant (α) for the upper and lower 2DEGs, respectively. Some αs for the upper 2DEG are lacked due to the insufficient FFT peak slitting. Note that the data for the two samples are plotted for $t_{QW} = 80$ nm.

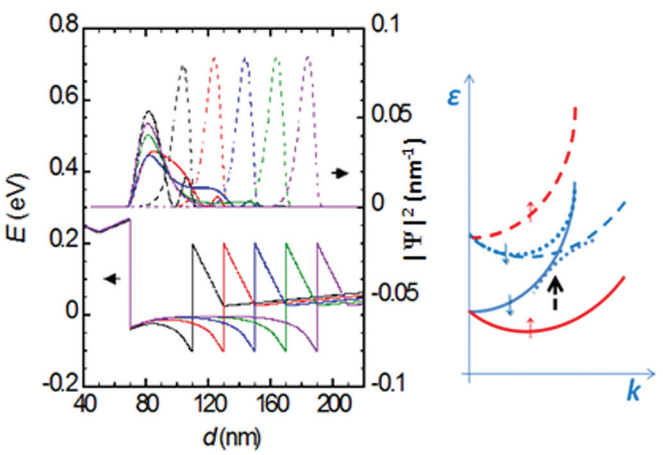


FIG. 6. (Left panel) Self-consistent calculation results of potential and spatial distribution of electrons in our 2DEG bilayer samples. Note here that the distributions of the upper (left) 2DEG in the narrow well samples ($t_{QW} \leq 80$ nm) seem to expand to the inside of the well suggesting the stronger interaction with the lower 2DEGs in those samples, although the coupling itself is not so tight. (Right panel) Schematic picture of anti-cross coupling between the spin-split dispersions of the upper and lower 2DEGs.

the precession motion would cancel out with each other, suggesting "apparent no spin-split" in the bilayer system itself. So that, even when the system is some extent asymmetric, the cancelling between the spin precessions would occur. This might suppress the overall SOI in the bilayer 2DEG system, even when there are no interactions between the 2DEGs. But, this simple picture is likely inconsistent with the experimental result obtained here for $\alpha$ by both the WAL and variable temperature MR measurements.

As seen in the left panel in Fig. 6, the electric field strengths, $\langle \boldsymbol{E}_y \rangle$, at the upper and lower interfaces seem almost the same for the five samples with different $t_{QW}$s. So that, the change of $\boldsymbol{E}_y$ does not seem to the main reason of the $\alpha$ enhancements. In addition, $n_s$ and m* have not changed so much depending on $t_{QW}$ enough to vary the $\alpha$ value. Thus, we again focus on the effect of $|\Psi|^2$ expansions in the narrow QWs, since it implies the super-position of $|\Psi|^2$ and then the tunneling between the upper and power 2DEGs. One candidate mechanism to enhance the $\alpha$ is thus the anti-cross coupling between the spin dispersions of the upper and lower 2DEGs[15,20] as schematically shown in Fig. 6, right panel. Since in our system, the same kinds of spin dispersions interact with each other, a strong mode coupling, which might bring about the dispersion deformation and hence the Rashba spin-splitting enhancement, would take place.

## IV. SUMMARY

In summary, we have fabricated bilayer 2DEG samples in a form of doubly modulation-doped wide $In_{0.75}Ga_{0.25}As$ quantum wells, the width of which are 40–120 nm. They were found to have high quality 2DEGs with the typical mobility of $\mu_e \leq 1.5 \times 10^5$ cm$^2$/V s for the total $n_s \sim 8 \times 10^{11}$/cm$^2$. The detailed parameter values such as $n_s$, the effective mass $m^*/m_0$, and the SO coupling constant $\alpha$ for each 2DEG sub-band were estimated successfully via variable temperature MR analysis.

Although the structure and doping condition are symmetric, $n_s$s are found to be asymmetric and the ratio of 1:3 ([upper]:[lower]) was confirmed. Relating to this result, lighter $m^*/m_0$ s in the upper 2DEGs than in the lower ones could be explained. Beyond the simple expectation, enhanced $\alpha$ were found for the samples with narrower QW widths in both the MR and WAL measurements. One possible origin is the result of interaction between the 2DEGs in the form of electron distribution super position suggested by the self-consistent calculation. The interaction in our case means implicitly the anti-cross coupling of the dispersion between the asymmetry and loosely coupled 2DEGs.

Fundamental spin transport properties confirmed here in the 2DEG bilayer, especially the very large $\alpha$ s ($\sim 20 \times 10^{-12}$ eV m) for both the upper and lower 2DEGs possibly interacting, seem to be promising to create a new class of spintronics devices based on the Rashba SOI.

## ACKNOWLEDGMENTS

This work was partially supported by JST ALCA (Advanced Low Carbon Technology R&D program) grant.

[1]*Semiconductor Spintronics and Quantum Computation*, edited by D. D. Awschalom, D. Loss, and N. Samarth (Springer, Berlin, 2002).
[2]H. Munekata, H. Ohno, S. von Molnar, A. Segmuller, L. L. Chang, and L. Esaki, Phys. Rev. Lett. **63**, 1849 (1989); H. Ohno, Science **281**, 951 (1998).
[3]S. Datta and B. Das, Appl. Phys. Lett. **56**, 665 (1990).
[4]Y. A. Bychkov and E. I. Rashba, J. Phys. C **17**, 6039 (1984).
[5]M. Schultz, F. Heinrichs, U. Merkt, T. Colin, T. Skauli, and S. Levold, Semicond. Sci. Technol. **11**, 1168 (1996).
[6]J. Nitta, T. Akazaki, H. Takayanagi, and T. Enoki, Phys. Rev. Lett. **78**, 1335 (1997).
[7]Y. Sato, T. Kita, S. Gozu, and S. Yamada, J. Appl. Phys. **89**, 8017 (2001).
[8]G. Engels, J. Lange, Th. Schapers, and H. Luth, Phys. Rev. B **55**, R1958 (1997); Th. Schapers, G. Engels, J. Lange, Th. Klocke, M. Hollfelder, and H. Luth, J. Appl. Phys. **83**, 4324 (1998).
[9]D. Grundler, Phys. Rev. Lett. **84**, 6074 (2000).
[10]M. Akabori, V. A. Guzenko, T. Sato, Th. Schapers, T. Suzuki, and S. Yamada, Phys. Rev. B **77**, 205320 (2008).
[11]S. Murakami, N. Nagaosa, and S.-C. Zhang, Science **301**, 1348 (2003).
[12]J. Sinova, D. Culcer, Q. Niu, N. A. Sinitsyn, T. Jungwirth, and A. H. MacDonald, Phys. Rev. Lett. **92**, 126603 (2004).
[13]J. Inoue, G. E. Bauer, and L. W. Molenkamp, Phys. Rev. B **70**, 041303 (2004).
[14]D. M. Gvozdic and U. Ekenberg, Appl. Phys. Lett. **90**, 053105 (2007).
[15]U. Ekenberg and D. M. Gvozdic, Phys. Rev. B **78**, 205317 (2008).
[16]T. Koga, J. Nitta, H. Takayanagi, and S. Datta, Phys. Rev. Lett. **88**, 126601 (2002).
[17]S. Datta, M. R. Melloch, S. Bandyopadhyay, R. Noren, M. Vaziri, M. Miller, and R. Reifernberger, Phys. Rev. Lett. **55**, 2344 (1985); S. Datta, M. R. Melloch, S. Bandyopadhyay, and M. S. Lundstrom, Appl. Phys. Lett. **48**, 487 (1986).
[18]Y. Aharonov and D. Bohm, Phys. Rev. **115**, 485 (1959).
[19]T. Z. Qian and Z. B. Su, Phys. Rev. Lett. **72**, 2311 (1994); J. Nitta, F. E. Meijer, and H. Takayanagi, Appl. Phys. Lett. **75**, 695 (1999).
[20]P.-Q. Jin and Y.-Q. Li, Phys. Rev. B **76**, 235311 (2007).
[21]D. R. Leadley, R. Fletcher, R. J. Nicholas, F. Tao, C. T. Foxon, and J. J. Harris, Phys. Rev. B **46**, 12439 (1992).
[22]S. Osako, T. Hamano, K. Yamasaki, K. Moriyasu, N. Mori, C. Hamaguchi, S. Sasa, and M. Inoue, Semicond. Sci. Technol. **13**, 181 (1998).
[23]T. Koga, J. Nitta, T. Akazaki, and H. Takayanagi, Phys. Rev. Lett. **89**, 046801 (2002).
[24]*Semiconductors and Semimetals,* Vol. 1, *Physics of III-V Compounds*, edited by R. K. Willardson and A. C. Beer (Academic, New York, 1977).
[25]K. Fujii, Y. Morikami, T. Ohyama, S. Gozu, and S. Yamada, Physica E **12**, 432 (2002).